Response to Anonymous Referee #2
(Received and published: 20 November 2009)
Final response of the authors to referee comment is in blue.

The manuscript presents a careful study of the BRDF of snow - probably one of the most accurate observations made to date. The results are compared to the predictions of two numerical models. Largely agreement is found and the small discrepancies are carefully discussed and explained. The paper is well-written and I suggest to publish the manuscript after consideration of the following minor points:

1/ Equation 1: In my understanding, F is not the radiance but the incident irradiance.The radiance of a collimated beam would be infinity anyway. Please check! This is confirmed by equation (2) because albedo is the ratio of reflected to incident irradiance.

We perfectly agree with this correction.
More details are given in response to specific comment 7 from Stephen Hudson.
Corrections have been implemented in the text.
Line 6/282 "to the incident irradiance of a collimated beam"
Line 17/282 "over the incident collimated irradiance at a given wavelength"

2/ Section 3.1: Please outline the significance of BRDF in contrast to HDRF (BRDF allows to calculate reflected radiance for any given incident sky radiance distribution while HDRF is in principle only applicable to the specific conditions during the observation)

We propose to modify the first paragraph of setion 3.1 (Line 11-15/283) into: '(…) Indeed most of the studies referenced below give access to HDRF and not BRDF. The latter allows to calculate reflected radiance for any given incident sky radiance distribution while HDRF is applicable to the specific conditions of illumination during the observation. (…)'

3/ page 19284, line 16: Please reference Stamnes et al. [1988] for DISORT
A reference to Stamnes et al. [1988] has been added line 16/284.

4/ page 19287, line 20: please replace by "symmetric with respect to the principle plane"! The "along the principle plane" made me think into the wrong direction.
Lines 19-20/287 have been modified into "In order to convert the BRDF measurements into spectral albedo and anisotropy factor, we assume that the BRDF is symmetric with respect to the principal plane (…)"
Detailed response is also given in the response to specific comment 11 from Stephen Hudson.

5/ page 19288, line 19: it is actually the "ice absorption bands", not the "water molecular absorption bands"; absorption properties of water vapour, liquid water and ice are completely different,

Line 19/288 has been modified into '4 secondary minima due to ice absorption bands'.

6/ page 19290, line 12: please make clear that each data point belongs to a different wavelength (?)

For clarity, we propose to add the following sentence in the legend of Figure 7: 'Each point on the charts belongs to a wavelength for one sample and one incident zenith angle '.

7/ page 19296, line 12: you might note that the 23 degree maximum is the well-known halo occurring for ice clouds with hexagonal columns

Indeed, the 23 degree maximum is responsible for the halo occurring for ice clouds with hexagonal columns. In order to understand, the origin of the double peak we make new simulations artificially increasing the imaginary part of ice refraction index. The results seem to indicate that the double peak is due to simple or multiple reflections at the surface of the grains without transmission through the grains.
A detailed response on the same subject can also be read in Hudson specific comment 23.
We propose to modify the text correspondingly (line 5/296).
" [...] the double peak may be caused by elongated forms or faceted crystals (dendritic crystals, cylinders, columns ...). Simulations have been done to investigate the origin of this double peak; Even with artificial increase of the imaginary refraction index of ice, the two maxima in the BRDF (at limb and at θv=30°, φ=180°) remain. This indicates that the double peak is due to simple or multiple reflections at the surface of the grains without transmission through the grains."

8/ Fig 5: It is actually "two wavelengths", not "several"

We perfectly agree with this correction. Legend of Figure 5 has been corrected consequently and now reads: "Ratio of the anisotropy factor R between samples S1 and S3 (R(S1)/R(S3)) at 0, 30 and 60° incident beam and for two wavelengths. The spectral albedo used to calculate R for S1 is indicated below the charts. S3 spectral albedo is indicated in Figure 4"
(See also suggested corrections 37 from Stephen Hudson).

Response to S. Hudson supplement #1
(Received and published: 24 September 2009)
Final response of the authors to referee comment is in blue.

General comments

This paper presents an overview of observations of the angular distribution of reflected radiance from natural snow samples, along with some comparisons of these observations to modelling results. The fact that the measurements were made under artificial light, allowing purely direct-beam incidence, makes them scientifically new and interesting. My main technical concern with the observations is related to the effect of the small sample size.

The issue of the sample size is discussed in detailed in our response to the specific comment 1.

I think the impact of the paper could be greatly extended through the inclusion of data at additional wavelengths and viewing angles. My first recommendation would be to resubmit the paper at a later date with an extended set of observations. This suggestion is based not on significant scientific flaws in the paper, but rather on the fact that the current dataset does not make the best use of the new possibilities made available by using the new laboratory observation system rather than field-based measurements. Therefore, it feels like an incomplete work that will have to be supplemented later. If the dataset extensions are for some reason not possible, or if the authors and editor choose to publish the current paper as a 'part one', it could be published after revisions to address the specific comments below.

We are very grateful to S. Hudson for its reviews which allow greatly improving the paper. More measurements have been performed than presented in the first version of the paper. We have chosen to present only a subset that was sufficient for the purpose of the paper, i.e. to exhibit the main features of the BRDF and relate them with the underlying physical processes.

In the new version we propose to include in the supplementary materials section, data of anisotropy factor for more wavelengths and for sample 2. In addition, the whole raw dataset is available upon demand from the corresponding author (mdumont@lgge.obs.ujf-grenoble.fr).

Proposed supplementary materials

Figure 1 - Ratio of the anisotropy factor R between samples S1 and S2 (R(S1)/R(S2)) at 0, 30 and 60° incident beam and for two wavelengths.

Figure 2 – S2 Anisotropy factor, R(θv ,φ) at 0.4, 0.6, 0.9, 1.0 and 1.5 µm. Incident angle is 0°. Data at 0.4 µm can only be used as anisotropy factor and not as absolute values of reflectance since calibration of the reference within 400-500 nm is not enough accurate.

Figure 3 – S2 Anisotropy factor, R(θv ,φ) at 1.8, 2.24 and 2.5 µm. Incident angle is 0°.

Figure 4 – S2 Anisotropy factor, R(θv ,φ) at 0.4, 0.6, 0.9, 1.0 and 1.5 µm. Incident angle is 30°.

Figure 5 – S2 Anisotropy factor, R(θv ,φ) at 1.8, 2.24 and 2.5 µm. Incident angle is 30°.

Figure 6 – S2 Anisotropy factor, R(θv ,φ) at 0.4, 0.6, 0.9, 1.0 and 1.5 µm. Incident angle is 60°.

Figure 7 – S2 Anisotropy factor R(θv ,φ) at 1.8, 2.24 and 2.5 µm. Incident angle is 60°.

Figure 8 - R(S3)-R(modelled) at 1.0 µm (SnowRAT, random cylinder, radius=0.4 mm, lenght=0.8 mm) and at 1.03 µm (Mishchenko model, spheres, same distribution as in the paper)

We agree that the data set collected is not an exhaustive sampling with all the wavelengths, and possible angles to be of general interest. However, these measurements are time consuming and a trade off was necessary to accommodate the availability of the instrument and to limit the duration of the measurement over each sample in order to avoid the metamorphose of the sample that would certainly degrade the interest of the measurements.

Our strategy, according to the goal of the paper, was to sample with a coarse angular resolution in order to be able to cover the whole hemisphere. It is clear that further specific measurements could be made in the future in order to answer specific questions (at a selected range of angles and/or wavelengths). However, it seems not possible to cover a wide range of wavelengths together with a fine angular resolution given the technical constraint and the risk of sample evolution during the measurement.

Specific comments

1. The snow sample that is observed is cylindrical, with a diameter of 30 cm and a depth of 12 cm. It is stated that this is "large enough to minimize side effects within a large range of wavelengths." Presumably, the large range of wavelengths is meant to include all wavelengths covered in the current work: from 500 nm. No reference or explanation is given for the statement that this is large enough to eliminate edge effects. A discussion in a reference given elsewhere in the paper (Brissaud et al 2004) refers to this issue, but it mostly addresses the question of errors caused by the finite size of the incident beam.

The effect of the loss of light to the sides and bottom of the cylinder should be discussed in more detail, along with a description of what is around the cylinder of snow. If the container holding the cylinder is white on the inside then it may have much less effect than if it is black (though it would still need to be examined, and the albedo of the sides given).

To investigate the potential problem, I used a Monte Carlo radiative transfer model that tracks photons through a cylinder of snow until they are absorbed, or leave the top, side, or bottom. Using the Henyey-Greenstein phase function and values of single-scattering albedo (1 minus 4x10-5) and asymmetry parameter (0.891) calculated for 400-micron-radius ice spheres using the ice optical properties given in Warren and Brandt (2008) for light with a wavelength of 600 nm, the model showed that 8.7% of the photons exited through the bottom of the cylinder and 5.0% through the side of the cylinder, while only 1.1% were absorbed. These results were for normal incidence ($\theta i=0°$) with all photons incident at the exact center of the top of the cylinder. The number of lost photons decreased some with increasing incident zenith angle, but remained 5.9% and 3.4% from the bottom and sides for $\theta i=60°$.

This model was obviously done as a quick check, and I am open to the possibility that I may have made an error in it. However, a similar result is seen in Figure 3 of Warren et al (2006), which shows transmission of about 10% of flux at 600 nm through 12 cm of snow in Antarctica, which has smaller grain sizes, giving a higher optical depth per unit of geometrical depth. Both of these results suggest the edge effects need to be much more thoroughly examined in the current paper.

During the design of the instrument and with the aim to conduct measurement of snow bidirectional reflectance at visible wavelengths, different experiments have been performed in order to investigate photon losses via side and bottom of sample (Brissaud et al., unpublished results). For these tests, artificial snow (grains size from 0.8 to 1.5mm) made of pure ice has been produced and sampled.
The results show that photometric errors of the system, compared to horizontally infinite homogeneous illumination are better than 0.2 % at 0° incident zenith angle, 70° viewing zenith angle and 630 nm.
These experiments have also been performed with a transparent cubic container (29.5 cm wide and 16.5 cm depth) to estimate losses at sides and bottom. At visible wavelengths, for a 4cm diameter circular lighting pattern (0° incident zenith angle), side loss is 0.5 % and bottom loss 1 %. An estimation of the impact of these losses on a 2 cm-diameter observation area is less than 0.1 %. Added to that the sides of the containers used for measurement of snow BRDF were made of a stainless steel plate (wooden bottom), consequently the mirror effect weakens the loss effects measured with the transparent cubic container.

In the quick model presented above, no impurities were considered. Natural snow always contains impurities that greatly reduce penetration depth in the visible range. In addition the asymmetry parameter chosen by the reviewer is probably higher than typical values for irregular ice grains as found in natural snow (0.7524 is used for irregular snow particle model in Mishchenko et al. [1999]). This might explain at least part of the discrepancies between the results of the model and the experiments quoted above.

We propose to include these data in the paper and to replace line 10-12 page 19286 by "The samples are cylindrical (…) and large enough to minimize edge effects even at visible wavelengths. Test experiments have been conducted at 630 nm on a transparent cubic sample holder (29.5x29.5x16.5cm^3) filled with artificial snow. The results show that side losses are less than 0.5% and bottom losses less than 1% at visible wavelengths and 0° incident zenith angle. Consequently photon losses in the 2 cm observation pattern are estimated to be less than 0.1%. The reflecting sides of the sample holder further decrease these losses."

2. One of the advantages of the laboratory measurements is the ability to measure something closer to the true BRDF, rather than the HDRF; i.e. to measure the reflection resulting from purely direct incident radiation. This advantage provides a reason to accept the risk of disturbing the snow by moving it to the lab. Unfortunately, no data are presented for the wavelengths where this advantage is most useful: the shortwave visible and ultraviolet. Field measurements made at wavelengths less than 500 nm are often dominated by diffuse incidence due to Rayleigh scattering, while the strong wavelength dependence of the scattering means that field measurements at longer wavelengths are made under a nearly direct beam. Using the SBDART atmospheric radiative transfer model to calculate the fraction of incident flux that is diffuse at sea level under a clear, subarctic winter atmosphere shows that, with a solar zenith angle of 60°, less than 25% of the incident flux is diffuse at wavelengths longer than 500 nm; less than 10% is diffuse at wavelengths longer than 630 nm, and less than 1.5% at wavelengths longer than 1 μm.

Given that the measurement under direct radiation is the main motivation given for the method, it seems very surprising that no measurements are presented at wavelengths between 300 and 500 nm, where up to 90% of the incident flux in the field may be diffuse. The

instrument description in Brissaud et al (2004) says it is capable of measurements down to 310 nm. Since it is the observations at shorter wavelengths that would provide the most scientifically interesting and new results here, I would suggest making those measurements and including them in the manuscript. If there is some reason that is not possible, then it should be explained here, and noted that it means that this method is currently limited to being used at the wavelengths where it provides the least advantage. Of course, the snow is even less absorptive at these short wavelengths, making the edge effects even larger, but it should not be much more significant than it is at 500 nm.

Indeed, measurements at wavelengths smaller than 500nm might be really new and interesting. In fact we performed measurements from 400 to 3000 nm for each sample and geometry. In the paper we only present results from 500 to 2500 nm since between 400 and 500 nm the reference panel (Spectralon) is not well calibrated (2% error) at these wavelengths. Additionally band-pass filters need to be used to remove unexpected wavelengths scattered inside the monochromatic source. At wavelengths smaller than 500nm, the monochromatic intensity produced by the source is very low and the relative contribution of unexpected wavelengths (without filtering) is then significant. Thus these unexpected wavelengths strongly contribute to the signal and largely alter the accuracy of the measurements. At wavelengths larger than 2500 nm, H_2O vapour absorption band at 2700 nm makes the measurements very noisy; that is why we have chosen not to present these inaccurate measurements in the paper.
As described in Brissaud et al. (2004), measurements are indeed possible from 310 nm but it requires more complicated setting and a longer duration of measurements.
We propose to include the results at 400 and 500 nm in the supplementary materials and in Figure 3 but only as anisotropy factor because the error due to the inaccurate calibration of the reference panel vanished in the calculation.

3. The choice to make observations at only 4 viewing zenith angles and 5 azimuth angles seems to limit the analysis. For example, in one case it was not possible to say whether a double maximum in the forward reflectance was present because it wasn't clear if there was one broad maximum, or if the minimum between the two maxima was not resolved. It also makes it difficult to interpret the double peak in reflectance when it is observed because one cannot say if the peak at $\theta v=30°$ is actually located at the location where specular reflection would be observed, or if it is actually at a slightly different angle, something which would be very helpful for interpreting the results. Having observations at $\theta v=80°$ and at azimuth angles of 5° to 30° would help to better understand the shape of the forward peak.

This is another case where the advantages of the laboratory setup do not seem to be fully used (field measurements typically have a wider observation field of view to be able to complete the measurements over the hemisphere before conditions change too much). I would be quite interested to see the detailed angular structure of the BRDF and comparisons of that with model results, but instead, I am left wondering whether the linear interpolation is really accurate, and I can only see a sort of general comparison. Measurements at finer angular resolution would also provide an argument for making observations at longer wavelengths, where the direct beam is less of a laboratory advantage. If observation time is a problem, then reducing the wavelength resolution from 20 nm to 100 nm would probably be fine, especially as only two wavelengths are presented.

See also response to specific comment 4.
Indeed, the chosen angular sampling is too coarse to see the details of the angular structure of the BRDF. This choice was motivated to limit the duration of measurement. Degrading spectral resolution does not significantly reduce observation time as the most limiting operation is the change of viewing and lighting angles due to detectors and mirror displacements.
The figure below presents a complementary scan made on S3 with a 10° angular sampling in the principal plane and compared with the results of a cos(θv) interpolation [for discussion on the impact of the interpolation of the measurement see response to specific comment 11]. Zenith incident angle is 30°.

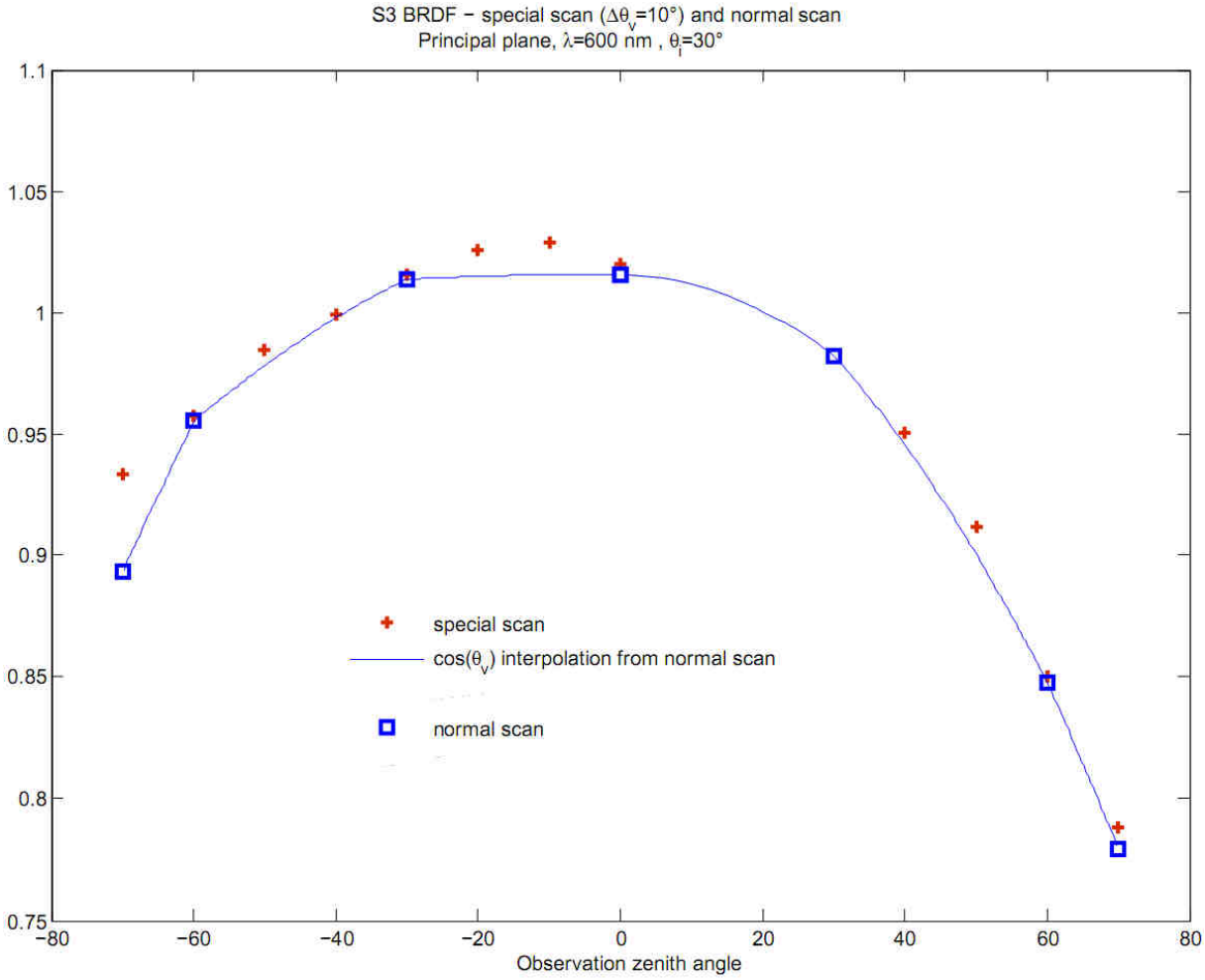

Figure 1

As shown in Figure 1, the interpolated curve calculated from the normal scan (i.e. coarse angular resolution) misses the maximum observed at -10° in the principal plane in the special scan (finer angular resolution). The impact of the interpolation in terms of accuracy is discussed in more details in the response to specific comment 11. In addition, the changes between the measurements of the normal scan and of the special scan in Figure 1

can be explained by the fact that the sample transformed between the two scans (there is a time interval of 14 days between the two scans).

As for the double peak observed at 1500nm, it would have been interesting to analyze the effect of the incident zenith angle. Unfortunately, we did not perform these measurements. Recently, after first submission of the manuscript, additional simulations have been made at 1500nm with SnowRAT using random cylinder with artificially increased imaginary refraction index of ice. This minimizes or even prevents the penetration of the photons inside the ice grains. The results shows the double peak (at limb and at 30° in the forward direction) still remain indicating that it results from a small (one or two) number of reflection events at the surface of the grains and not due to transmission through the grain.

4. Also, it would seem useful to include larger incident zenith angles (70° and 80°), since these are common over snow and are most affected by diffuse incidence in the field.

Measurements at grazing angles are limited by the size of the container. Indeed, edge effects (loss or unexpected reflections on the side on the container) would be significant. Measurement at 70° incident zenith angle seems possible but significant correction has to be developed.
Additional details are given in the response specific comment 3.

We suggested adding in the text line 3/287:
"Measurements at larger incident or observation zenith angles were not performed since edge effects due to the size of the sample holders are too significant for these configurations".

5. Despite the large set of measurements, observations from only two wavelengths are shown. It would be interesting to include those from some other wavelengths as well, especially for comparison with the modelling results. Given that the modelling results are for comparison with the observations, it is not very useful to show results from the model for wavelengths that are not also shown in the observations. Also, including the full dataset, or a more extensive subset of it, as supplementary material would be useful to others who wish to make use of this work.

In the paper, we prefer to present two different wavelengths (600 and 1500 nm) for which the BRDF are different owing to the difference of absorption coefficient.
Results at some other wavelengths are included in the supplementary materials section: 0.4, 0.6, 0.9, 1.0, 1.5, 1.8, 2.24 and 2.5 μm.
We also propose to add line 13/280 "The whole dataset is available on demand from the corresponding author."

6. In Sections 1 and 2 (particularly line 26, page 19280), Nicodemus et al (1977) seems to be the defining reference for reflectance terms, including BRDF, bi-conical, hemispherical-directional, etc.

Reference to Nicodemus at al (1977) was added line 26/280, line 8/281, line 16/282, line 22/282, line 7/282 and line 8/283.

7. In the discussion of equations 1 and 2, at lines 6 and 17 on page 19282, the denominator being discussed [F(θi, φi, λ)] is the incident flux (or irradiance), not radiance or intensity. It is the radiance times the cosine of the incident zenith angle.

Corrections have been implemented in the text.
Line 6/282 "to the incident irradiance of a collimated beam"
Line 17/282 "over the incident collimated irradiance at a given wavelength"

8. Line 11, page 19284, perhaps cite Wiscombe and Warren (1980) since Warren and Wiscombe (1980) was part II and included impurities, something not discussed here.

We have modified line 11/284.

9. In section 4.3, since the definition of BRDF was given precisely, it should be noted that what is actually measured is the directional-conical reflectance factor, since the observation is not for an infinitesimal solid angle.

To be inserted line 7/286.
"As noticed in [Schaepman-Strub et al. 2006], BRDF as defined in equation [1] cannot be directly measured since it requires an infinitesimal solid angle of observation. Thus the quantity measured by the spectrogonio-radiometer is the directional-conical reflectance. Nevertheless since the detector field of view is small we consider in the following that our measurement are very close to BRDF."

10. Line 18, page 19287, the quantity in the second set of parentheses should have θi ≈ θv.

The text has been corrected line 18/287.
"As the incident beam, (θi ≈ θv,..)"

11. At the end of page 19287, it says linear interpolation was used to cover the whole hemisphere. a) Was it linear in θv or μv? It's not clear which is better, but often the latter is more physical, and it should be stated which was used.

The original interpolation was linear in θv. The figure below shows the two interpolations for S3 at 1500 nm and 30° zenith incident angle. On the two charts, the polar axe 'r' is linear in θv.

Interpolation linear in θv	Interpolation linear in μv
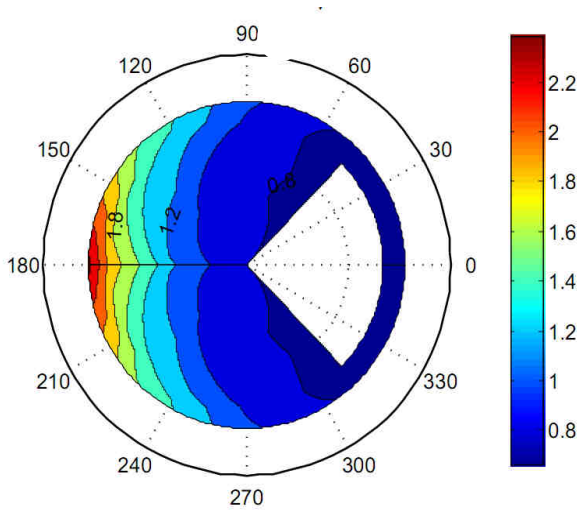	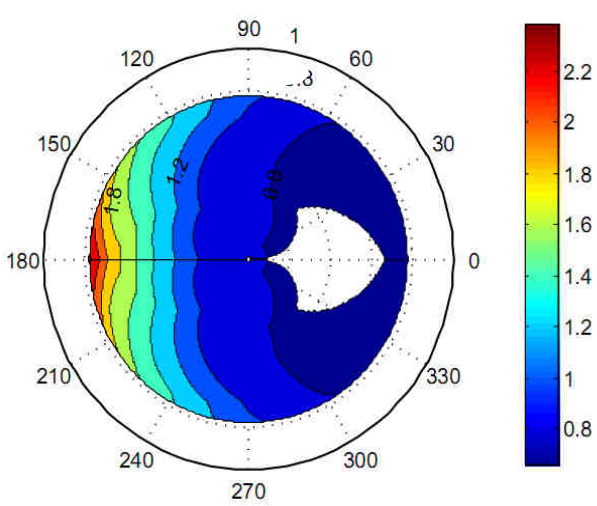

Figure 2

Figure 2 shows that discrepancies are small between the two interpolations, difference only reaches 0.05 at some points. However, R isolines seem more physical in the case of μv interpolation. Furthermore, considering the interpolation shown in Figure 1 (μv interpolation), we can infer that using interpolation linear in θv is slightly less accurate than using μv interpolation. Thus, we have decided to use interpolation linear in μv in the new version of the paper. The figures are modified accordingly.

Added in the text:
Line 21/287
"In order to convert the BRDF measurements into spectral albedo and anisotropy factor, we assume that the BRDF is symmetric with respect to the principal pane (Hudson et al., 2006) (for azimuths from 180° to 360°) and perform a linear interpolation in cos(θv) and Φ for our measurements over the whole observation hemisphere."

b) Filling the hemisphere would require extrapolation as well as interpolation, which should be stated for clarity.
Extrapolation is indeed performed to calculate the spectral albedo.
1/ For all the incident zenith angles, an extrapolation is performed to extend the measurements from θv=70° in the range 70°-90°. Since the shape of the BRDF is unknown in this range, we assume it to be constant from 70° to 90° to compute the spectral albedo. The impact of this assumption is small since the ring from 70° to 90° contributes to only 11% ($1/2*\cos(70)^2=0.0585$) of the whole hemisphere in terms of projected solid angle.

2/ The second extrapolation performed to compute spectral albedo is filling the blank in the data due to shadow of the detectors on the sample in the principal plane. In the case of incident zenith angles of 30° and 60° we have chosen to use the measurements at Φ = 45° to extrapolate the data in the principal plane.

At nadir incidence, Φ = 45° is not measurable. Hence, we assume the data to be constant from θv=30° to θv=0°. This assumption may result in an underestimation of the spectral albedo.

c) Is it possible to estimate the uncertainty in the calculated albedo, due to the interpolation?

The uncertainty resulting from the interpolation (μv) discussed in comment 11.a and extrapolation in comment 11.b is estimated below.

In order to estimate the uncertainty in the calculated albedo, we use simulated BRDF from Mishchenko model with spherical grains. The model gives BRDF values with a 2° resolution in both incidence and azimuth angles. We first calculate the simulated spectral albedo (α_simul) by integrating the BRDF at this resolution and we compare it with:

. α_interp : spectral albedo calculated from simulation values taken at the same angles as the measurements, then interpolated in μv and extrapolated as constant from 70° to 90°

. α_thetai : where theta_i takes the value of each incident zenith angles (0,30 and 60°). Spectral albedo computed as α_interp but with an additional extrapolation due to data blank (shadow of the detectors, explain in comment 11.b) depending on theta_i.

The latter is the most representative of the measured one while the first is the closest to ideal case.

Table 1 – Estimation of spectral albedo accuracy using Mischenko model

	α_simul	α_interp	α_thetai
Θi=0°,600 nm	0.9708	0.9675	0.9608
Θi=30°,600 nm	0.9715	0.9771	0.9770
Θi=60°,600 nm	0.9786	0.9943	0.9673
Θi=0°,1020 nm	0.6530	0.6497	0.6410
Θi=30°,1020 nm	0.6732	0.6773	0.6772
Θi=60°,1020 nm	0.7461	0.7651	0.7388
Θi=0°,2000 nm	0.0783	0.0731	0.0725
Θi=30°,2000 nm	0.0891	0.0915	0.0930
Θi=60°,2000 nm	0.1557	0.1504	0.1458

In Table 1, one can infer that the maximum error is 1.8% up to 1020nm. We have to keep in mind that these simulations are for spheres and that the results might be slightly different for natural snow.

We performed the same analysis using cylinders (0.4mm) and the SnowRAT, model and the results are of the same order of magnitude and are gathered Table 2.

When absorption is more important (e.g. at 2000nm in Table 1), the relative difference is more significant. However this might be due to the fact that spheres are considered and caused the rainbow in the backscattering direction, which becomes more important in magnitude at more absorbing wavelengths.

Table 2 – Estimation of spectral albedo uncertainties using SnowRAT

	α_simul	α_30°
Θi=30°,1000 nm	0.5187	0.5132
Θi=30°,1300 nm	0.2117	0.2108
Θi=30°,1500 nm	0.0063	0.0055

We have also compares the impact of μv or θv interpolation in the case of spheres with Mishchenko model. The difference between spectral albedos from the interpolation is less than 0.05 % for all the cases listed in Table 1.

Nevertheless, the last effect to be noticed is that at 60° and 30°, the coarse resolution of the angular sampling in azimuth might lead to overestimate the angular width of the specular peak which can imply an overestimation on the calculated spectral albedo. This issue cannot be simulated using spheres and Mishchenko's model. Instead SnowRAT shows that at 30°, 1500 nm and for cylinders the spectral albedo is not overestimated.

This study leads us to conclude that the uncertainties due to the interpolation and extrapolation of the measurements are:
. less than 2% at wavelengths except near the absorption bands;
. higher in percentage at absorption maximum (1.5 and 2 μm) ~ 0.002 in reflectance value. Nevertheless, at absorption maximum, spectral albedo values are very low (often less than 0.01) and even reached the absolute accuracy possible with the instrument.

See also response to specific comment 29.

d) If ρ were reported, rather than R, then it would not be necessary to use the calculated albedo, which may be in error due to having measurements at relatively few viewing angles.

We agree that reporting ρ instead of R avoid the uncertainties in the calculated spectral albedo. However, reporting ρ instead of R makes the comparisons difficult between samples, wavelengths and incident angles because the range is much larger. Consequently, we propose to keep R on the charts but to indicate for each chart the value of spectral albedo used to generate R. This way, comparisons are easier and calculating back of ρ is possible.
Furthermore, reporting R instead of ρ avoids possible uncertainties due to reference calibration (this is especially useful at wavelengths smaller than 500 nm).

Considering specific comment 11, we proposed to modify line 19-22/287 into "In order to convert the BRDF measurements into spectral albedo and anisotropy factor, we assume that the BRDF is symmetric with respect to the principal plane (…) and perform linear interpolation (in cos(θv) and Φ) of the measurements. Extrapolation of the measurements have also been performed firstly from 70° to 90° observation zenith angle for all the incident zenith angles and secondly to fill the blanks due to the shadow of detectors.
Results of simulation with Mishchenko's model (Mishchenko et al., 1999) and SnowRAT model (Picard et al., 2008) have shown that the uncertainties of the spectral albedo values resulting from interpolation and extrapolation is less than 2% except at very high absorption value i.e. spectral albedo smaller than 0.01. An estimation of the resulting uncertainties has been plotted in Figure 3. Spectral albedo values used in R charts are indicated in the legend of each figure."

12. Line 2, page 19289, the larger absolute deviations of R from unity are in the forward-scattering direction. However, the relative difference may be nearly as large in the backscattering direction.

Line 2/289 "especially in the backscattering direction" has been removed

13. Line 6-7, page 19289, at nadir incidence, R should be circularly symmetric (varying only with θv), not only symmetric with respect to the 90-270 axis.

Line 6-7/289 has been reformulated "the anisotropy factor is not fully circularly (varying only with θv) symmetric as it should be for perfectly horizontal sample"

14. Line 22, page 19289 says "At 1.5 μm, the variations of R(S1)/R(S3) are stronger at 30° than at 60° incident angle." This doesn't really seem to be true; the maximum value is larger at 30° (1.8 versus 1.4), but the variability in the side and backward directions is larger at 60° (0.5 compared to 0.8), and a ratio of 0.5 is as different from 1 as a ratio of 2, so the difference is a bit more complicated than explained in the text. Also, the maximum values in the forward peak at 60° are likely not observed, so the ratio might get larger there if observations extended to 80° viewing angle.

We propose to replace line22/289 by "At 1.5μm, the variability of R(S1)/R(S3) seems to be larger at 60°, especially in the side and backward directions. As for the forward direction, the maximum value is larger at 30° but the ratio might be larger at 60° if observations were extended at 80° viewing angle".

15. Lines 24-25, page 19289, what does 'sharper and higher' mean? Why is it stated that the observed differences are definitely due to the grain size, when it is acknowledged elsewhere that grain shape can also be important?

'sharper' means less angular area extent ; 'higher' means higher in magnitude.

We propose to replace line 23-25/289 by "Moreover, concerning R(S1)/R(S2), the variability of the ratio increases with incident zenith angle and seems to indicate that for small and elongated grains, the forward scattering peak is higher in magnitude than for large rounded grains."

We also propose to add the ratio R(S1)/R(S2) in the supplementary materials.

16. Section 7.1, was it really a power law distribution that was used? If so, were there some limits placed on the range of sizes, since an unrestricted power law would make a lot of very small particles? A log-normal distribution, or something similar, seems more common for size distributions.

The size distribution used for the simulation in section 7.1 is a power law distribution as presented in Mishchenko et al. 1999, page 414. We imposed an effective radius and an effective variance and maximum and minimum radii are calculated automatically. We have added the precise reference in the text line 7/291.

17. What shape and size were the cylinders used in the SnowRAT model. The effective radius is given, but what was the radius and length of the cylinders?

The cylinders used in the SnowRAT model are as follow:

1/ 0.4 mm radius and 0.8 mm length

2/ 1mm radius and 2 mm length

Titles in Figure 9 has been corrected accordingly.

18. Lines 2-3, page 19292, the darkening at grazing angles also appears in the model at 1.3 μm (maybe at 1.5 also, but no details are visible there).

The formulation has been corrected in the text. Line 2-3/292 now reads "darkening at grazing angles appears at 0.9,1 and 1.3 μm".
At 1.5 μm, there might be no darkening at grazing angle since absorption is very high and the contribution of multiple scattering to the total reflected radiance might be negligible.

19. The reference to Aoki et al (2000) in line 25 of page 19292 should be replaced with Warren and Brandt (2008), which is a review and compilation of work done since Warren (1984), the main source for Aoki's figure.

The reference has been changed line 25/292.

20. Line 15 of page 19293 refers to Figure 3a of Hudson et al (2006); in that figure, the darkening at grazing angles occurs only at non-forward directions—there is still a forward peak near the horizon.

Line 15/293 has been reformulated into "the effect is noticeable as well in Fig. 3a in Hudson et al. (2006) but only at non-forward directions."

21. I found the discussion of the source function in the paragraph going from page 19293 to 19294 confusing. I think it could be clarified in general. One specific point about the statement "the source function decreases from the surface to depth because downward diffuse radiation approaches zero close to the surface"—my understanding was that the source function generally decreases with increasing depth, but that in the uppermost layer it increases with depth because of the lack of diffuse radiation right near the surface. That is, the source function initially increases with depth from the surface, reaches a maximum at a small depth below the surface, and then steadily decreases with depth. Then the reduction in radiance as you look at very large viewing zenith angles is due to looking into the region above the maximum in the source function.

We propose to replace line 21-28/293 by « The source function generally decreases from the surface to depth, except in the uppermost layers where it increases with depth because downward diffuse radiation approaches zero very close to the surface. Thus the source function initially increases with depth from the surface, reaches a maximum just below the surface and then steadily decreases. Consequently at grazing observation angles, the energy emerges from the region located above the maximum in the source function. Thus radiance is lower than at near vertical observation angles in which case the energy emerges from the region located deeper in the snowpack, including the maximum of the source function».

22. Case 2 in Section 8.1, the forward scattering peak, is also observed for short (low-absorption) wavelengths with large enough incident zenith angle. Line 15 on page 19294 should read something like, "At large incident zenith angles, or at wavelengths with strong

absorption, R patterns show a strong forward scattering peak." Also, line 6 on page 19295 should read something like, "2) strong absorption or high incident angle…."

With weak absorption, the forward scattering peak will still show up at large incident zenith angles (as seen in Figure 4c) because part of the forward peak of the phase function then sends photons toward the surface in the forward peak direction, so even though multiple scattering is possible, the photons are still progressively more likely to exit in the forward direction.

Line 15/924 has been reformulated to "At wavelength larger than 1 μm or at large incident zenith angle…"
Line 6/295 now reads "2) strong absorption and/or high incident angle….".

23. In the paragraph starting at line 5 on page 19296, it is not clear how a peak in the phase function at 22-25° would cause a peak in R at about (θv=30°, φ=180°). With the incident zenith angle of 30°, that viewing angle requires a deviation of 120°, so that is the angle where a peak in the phase function would explain the peak in R, but 120° is often a minimum in Xie's phase functions.

We acknowledge that our explanation is confusing. To investigate the issue we have performed new simulations by artificially increasing the absorption. These simulations indicate that the double peak may solely involve single or multiple reflections at the surface of the grains and no transmission through the grains.
We propose to modify the text into:
" [...] the double peak may be caused by elongated forms or faceted crystals (dendritic crystals, cylinders, columns ...). Simulations have been done to investigate the origin of this double peak using cylinders. Even with artificial increase of the imaginary refraction index of ice, the two maxima in the BRDF (at limb and at θv=30°, φ=180°) remain. This indicates that the double may solely involve single or multiple reflections at the surface of the grains without transmission through the grains."
See also specific comment 3.

24. In the last paragraph of Section 8.2, it seems unlikely that diffuse illumination hides the double peak in field observations at 1.5 microns since there is essentially no diffuse illumination under a clear sky at such a long wavelength. I would expect the second explanation (that measurements are typically made with larger solar zenith angle), or the angular field of view of the field sensors to be the cause for this not being observed in the field.

We agree with the comment. Line 15-16/296 has been modified: "The double peak has rarely been measured in the past since angular field of view of the field sensors is typically too large. In addition…"

25. Line 17 of page 19297, forward scattering is also stronger for shorter wavelengths with larger incidence angle.
See also specific comment 22.
Line 17/297 now reads "for wavelengths longer than 1 μm or/and large incident zenith angles"

26. In the conclusions (line 26 page 19297) it states that using non-spherical shapes for the grains improves the agreement between the measurements and model, but it is not clear that this is the case from the results presented here. First, there is only one case, 1.5 microns with incident angle 30°, that can be compared between observations and both models, so any such conclusion appears to be generalized from one point. Second, looking at that case, except for the rainbow, the results in Figure 8c look a lot more like the observation in Figure 4d than the results in Figure 9g or h do. Therefore, while it is probably true that using non-spherical shapes can improve the agreement, it is not shown here.

A comparison between measurements and models at 1.0 and 1.03 µm has been added in the supplementary materials (see Figure 3 below). It shows that discrepancies between models and measurements seem smaller for cylinders than for spheres. This fact is less obvious at 1.5 µm.

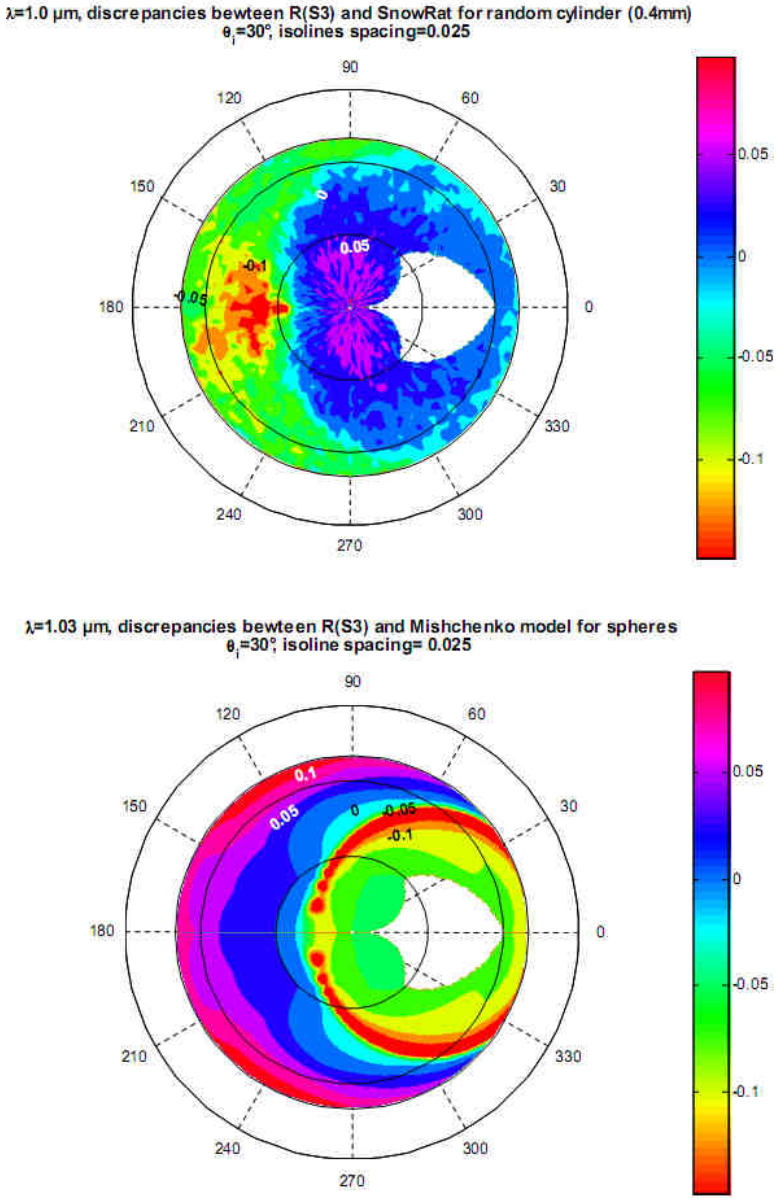

Figure 3

We authors propose to replace lines 26-27/297 by: 'Using non-spherical shapes allows to simulate feature as the double peak, avoid artefact such as rainbow that appears for

spheres and probably contribute to better agreements between models and measurements at 30° incident zenith angle for 1.0 and 1.03 μm.'

27. In Table 1, should the SSA for S2 be 126 m2 kg-1? That would be the more standard units and gives a radius of about 25 μm, while the current units seem to imply a radius of about 0.4 m.

Thank you for spotting this error in Table 1. We corrected with "SSA=12.6 $m^2 kg^{-1}$" which gives an optical radius of 250 μm.

28. Figure 1 would be clearer if the horizontal plane at z=0 were shaded to show the surface. The negative z axis is not needed and the reference surface would help show which lines are projected on the surface, and which are above it.

In the text, φ is generally used as the angle between the incoming and reflected azimuths, but here it is an absolute direction.
Offsetting the value of z where the θ arcs intersect the z-axis would make it clear that they are two different arcs.
Figure 1 has been accordingly modified. Please refer to the new figures at the end of this response.

29. The spectral albedos plotted in Figure 2 need to be discussed. The values at 0° and 30° incidence seem surprisingly low, compared to Wiscombe and Warren (1980), for example. Perhaps it could be explained by impurities. Also, the increase in albedo in the visible from 30° to 60° seems too large. Models, such as Wiscombe and Warren (1980), show little effect of zenith angle on albedo at non-absorbing wavelengths. Also, extrapolating that increase to larger incident zenith angles gives albedos well over 1. Perhaps calculating the albedo from a small number of radiances that do not cover all angles leads to some of these unusual features.

1/ It appears that in Figure 2, albedos were computed using a too coarse angular grid to interpolate accurately the function g(θv)=sin(θv)cos(θv) which implied a bias of 8% due to the high non linearity of g(θv). We have refined the angular grid to reduce this uncertainty (see specific comment 11).
The new computed spectral albedos are then presented below:

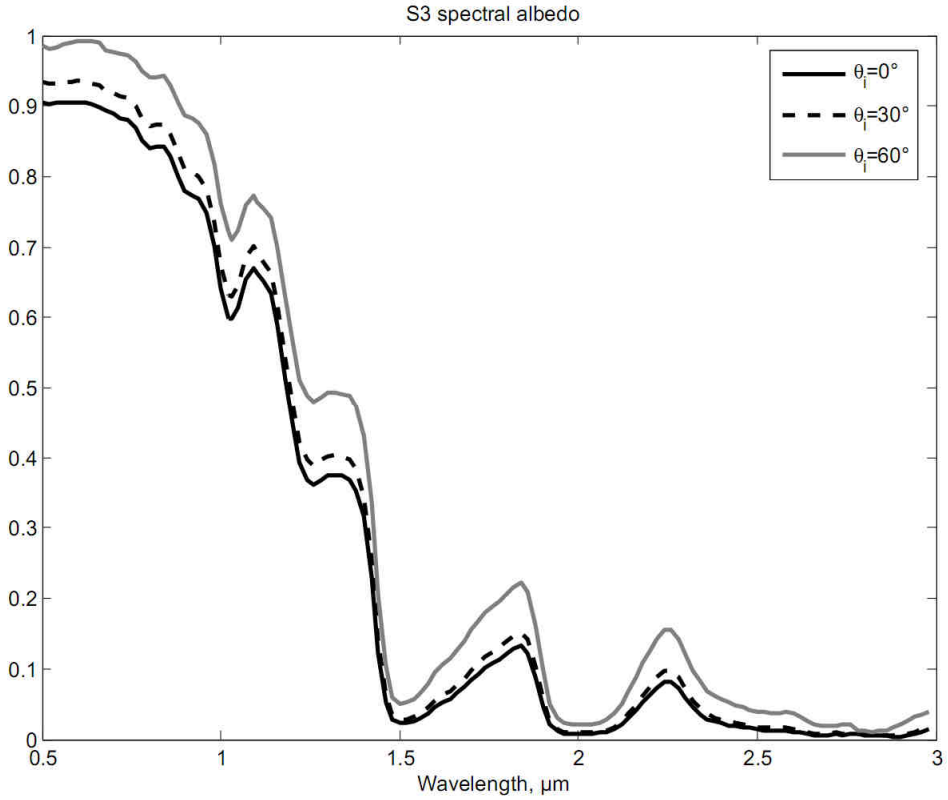

Figure 4

At visible wavelengths and nadir incidence, albedo is slightly higher than before (0.9054 at 600nm). Our values are low compared to those expected for pure snow. However, snow was sampled near manned areas and contains significant amount of impurities. This likely explains the low values as described in the following.

2/ To explain the unusual features presented in the paper Figure 2, we performed spectral albedo simulations using DISORT (Stamnes et al [1988]) for pure snow (ice spherical grains) and for snow contaminated with mineral dust or with soot. Refractive indexes for soot and dust comes from GEISA (LMD/Polytechnique) database and we studied the effect of impurities on spectral albedo versus incident zenith angle. Spectral resolution is rough (100 nm) but sufficient for the purpose of the discussion. Results are plotted in Figure 5 and 6.

See also response to specific comment 11 for the impact of interpolation and extrapolation on spectral albedo values.

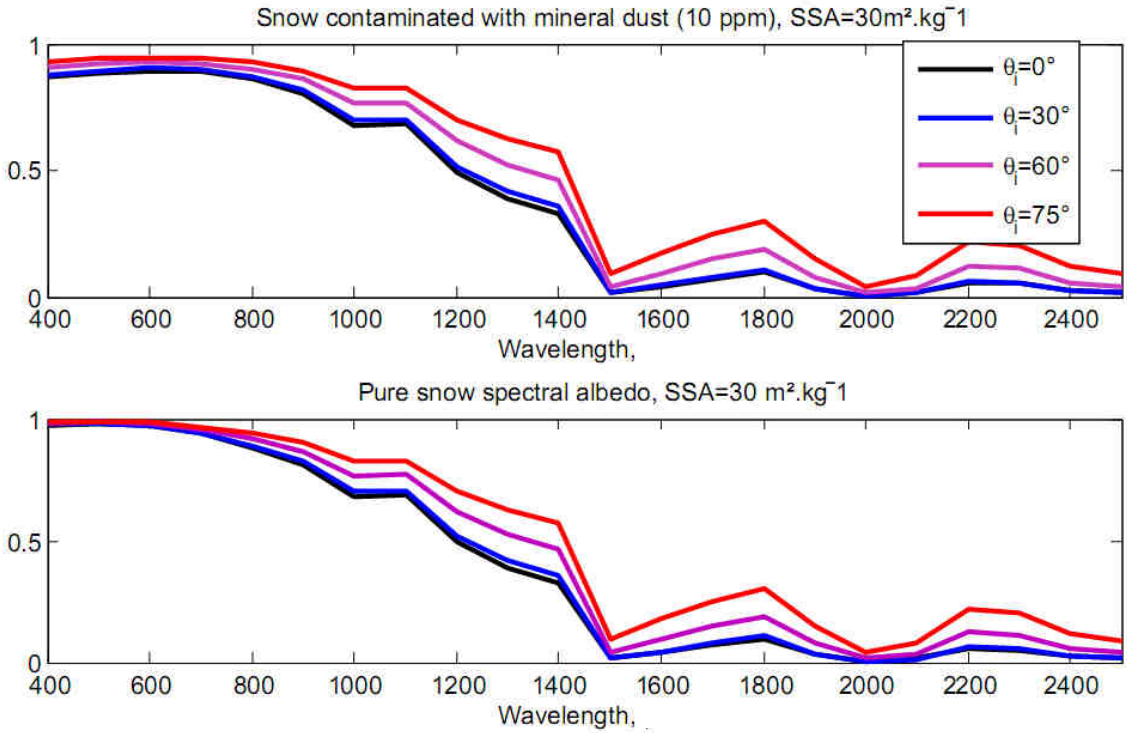

Figure 5

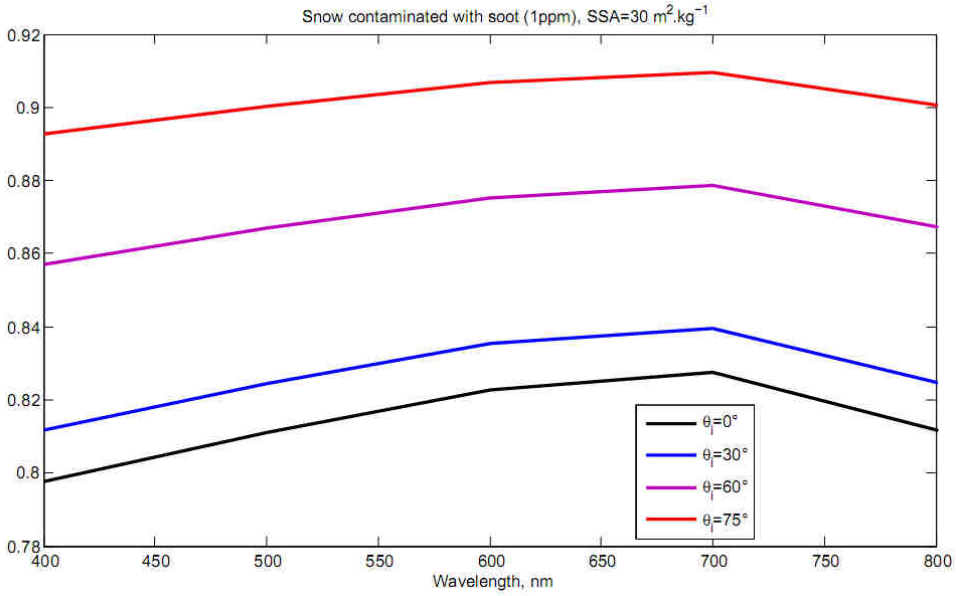

Figure 6

These plots show that for snow containing impurities the dependence on the incident zenith angle is higher than for pure snow even at visible wavelengths. The increase of the albedo

from 30° to 60° is higher that from 0° to 30°. DISORT simulations also show that the higher the content in impurities the higher the increase due to incident zenith angle is.

Figure 6 below shows spectral albedo calculated for the tree samples. Visual inspection of the sample indicated that c(S1)~c(S3) << c(S2) where c is impurity concentration in the snow sample. This observation is consistent with the results of the measurements (Table below).

Table 3 – Spectral albedo calculated from BRDF measurements, at 600 nm

	0°	30°	60°
S1	0.902	0.9287	0.9758
S2	0.8396	0.8811	0.9585
S3	0.9054	0.9352	0.992

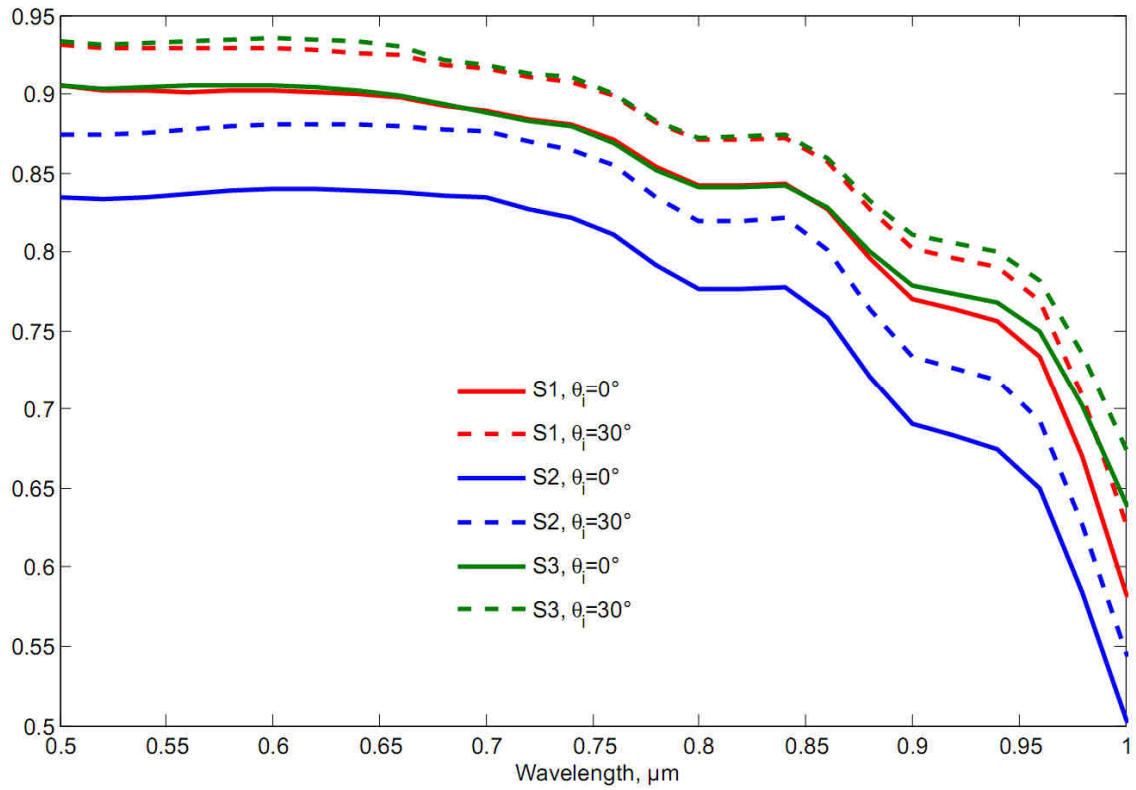

Figure 7 – Sample spectral albedo at 0° and 30° incident zenith angle

3/ The values at 60° might be slightly overestimated by 1 or 2 % due to the overestimation of the specular reflection as explained in response to specific comment 11.c/.

As for the extrapolation of the results for incident zenith angles higher than 60°, we believe that for low impurity content if the incident zenith angle is high, the behaviour is the same as if there is no impurity. Indeed, for very high incident zenith angle, the length

of the optical path of a photon before escaping the snowpack is small enough to limit the probability of being absorbed.

Considering these results we propose to add line 21/292: 'Furthermore, as noticed earlier, spectral albedo increases with incident zenith angle at all wavelengths including visible wavelengths. This quite unusual feature is most probably due to the fact that snow sample contain impurities. Thus visible wavelengths present the same pattern as more absorbing wavelengths due to absorption caused by impurities. It largely differs from the behaviour of pure snow which is highly transparent at visible wavelengths."

30. In Figures 4, 5, and 6, the interpolation between θv=30° and θv=0° could be done for all azimuths; there is no reason that the observation at θv=0° should be viewed as only being at an azimuth of 0°.
For the θi=30° observations, why are there no data for θv=60° or θv=70°, with 0° azimuth (i.e. no data in the backward direction)?
Similarly for θi=60°, I would expect to see data in the backward direction at θv=30°, and maybe also at θv=70°.

There was a default in the plot routine (θv was only varying into [45,180]). The error has been removed and Figures 4, 5 and 6 are corrected. Nevertheless, there is no data point for θi=60°, θv=70° in the backscattering direction since the detector would shadow the surface of the sample in this configuration (instrument issue).

The contours lines in the areas that are shaded white, or nearly white, should be made black or dark gray. This applies most to the contour for R=4 in Figure 4f.

Figures have been accordingly modified.

31. The average value of R over the hemisphere (weighted by cosθv and dω) should be 1, yet in Figures 8a and b there are few, if any, values greater than 1. What is happening there?

There was a default in the plot routine. We did not divide reflectance results by cos(θi) (= 0.866 for 30°). Many thanks for pointing this important error. All the plots are now divided by 0.866. This way the average value of R is 1. Figure 8 have been modified.

32. If the values in Figures 9g and h really vary so much that the current versions of the plots are correct, then they need to be plotted with a different colorbar that allows the variations of R to be seen. Using one consistent colorbar is nice, when possible, but in this case it makes it impossible to examine the results.

Figure 9 has been consequently modified and two different colorbars are now used.

33. Since the main point of the modelling is for comparison with and to help understand the observations, it would be useful to plot the differences between the model and the observations (possibly in addition to the plots of the modelled R). The comparisons by eye are difficult to make.

These plots are added in the supplementary materials.

Suggested Corrections

All the corrections suggested bellow has been done in the text.

1. 4/280 (line 4, page 19280): ‘one of the first sets’
2. 19/281: ‘They are also one of the first investigations’
3. 20/281: ‘configurations’
4. 22/281 and elsewhere (search phenomenons): the plural of ‘phenomenon’ is usually ‘phenomena’ **(also 1/291, 20/291 and 10/293)**
5. 3/282: ‘top of atmosphere’ does not need to be capitalized
6. 11/282: replace ‘supposed’ with ‘assumed’
7. 21/282: change to ‘R(θi, φ, θv, λ), a normalized BRDF value, is often used.’
8. 2/283: begin a new paragraph at ‘In most field…’
9. Equation 4: the subscript ‘o’ in the denominator should be ‘i’ for consistency
10. 12/283: ‘properties have been performed’
11. 23/283: ‘field measurements’ (no s on field)
12. 5-6/284: ‘studies illustrate the main patterns’
13. 24/284: change ‘lead’ to ‘led’ if you want to use the past tense, or ‘leads’ to use the present tense
14. 2/285: ‘are more appropriate for simulating snow’
15. 2-3/286: ‘At nadir incidence, the illumination pattern at the sample surface is circular, with a 200 mm diameter.’ (Otherwise it says it is always circular, but the diameter changes)
16. 17/286: delete the ‘d’ from ‘refrozed’
17. 18/286: delete the ‘s’ from ‘grains’ (could also add an apostrophe after the s, grains’, to make it possessive, but ‘grain shape and size’ would sound most natural to me)
18. 24/286: change ‘have’ to ‘has’; it goes with ‘a set’, singular
19. 3/288: delete ‘d’ from ‘changed
20. 9/288: change ‘minima’ to ‘minimum’
21. 22-23/288: ‘as a function of wavelength, for three different observation angles, with a fixed illumination angle’ (the values in figure 3 are plotted as a function of wavelength)
22. 8/289: change ‘-30° viewing zenith angle’ to ‘30° viewing zenith angle, in the forward direction’ or something like that.
23. 5&6/290: change ‘maxima’ to ‘maximum’ (singular) 24. 7/290: change ‘maximum’ to ‘maxima’ (plural)
25. 21/290: change ‘is’ to ‘are’ (refers to ‘sizes’); add a comma after ‘1 mm’
26. 4/292: ‘maxima’ -> ‘maximum’
27. 24/293: change ‘ends’ to ‘tends’
28. 4/294: delete ‘e’ in ‘occurs’
29. 5/294: change ‘S. J.’ to ‘S. G.’ (assuming it refers to Steve Warren, Seattle)
30. 16/295: change ‘differ’ to ‘differs’ (refers to ‘ratio’)
31. 6/296: I think this should be Figure 6a; Figure 4 is for S3, not S1
32. 21/296: ‘maxima’->’maximum’
33. 22/296: change ‘illuminate’ to ‘illuminates’
34. 21/297: delete ‘factor’; the anisotropy factor increases in some viewing angles and decreases in others, but the overall anisotropy increases
35. 9/298: change ‘for its comments’ to ‘for her comments’
36. Table 1, footnote b: ‘Specific Surface Area (total surface of ice crystals accessible to gas, per unit mass of ice) was measured for S2 using the methane absorption method (Legagneux et al., 2002).
37. Caption for Figure 5: change ‘several’ to ‘two’
38. Figures 8 and 9: add a polar angle (θv) grid **. Polar circles at 30, 60 and 70° have been added on the charts to allow easy comparisons with the measurements.**

References used in this review that are not in the manuscript **Added in the text**

Nicodemus, F. E., J. C. Richmond, J. J. Hsia, I. W. Ginsberg, and T. Limperis (1977), Geometrical Considerations and Nomenclature for Reflectance, NBS Monogr., vol. 160, Natl. Inst. of Stand. and Technol., Gaithersburg, Md (available at http://graphics.stanford.edu/courses/cs448-05-winter/papers/nicodemus-brdf-nist.pdf)

Warren, S. G., and R. E. Brandt (2008), Optical constants of ice from the ultraviolet to the microwave: A revised compilation, J. Geophys. Res., 113, D14220, doi:10.1029/2007JD009744.

Warren, S. G., R. E. Brandt, and T. C. Grenfell (2006), Visible and near-ultraviolet absorption spectrum of ice from transmission of solar radiation into snow, Appl. Optics, 45, 5320—5334.

New proposed figures

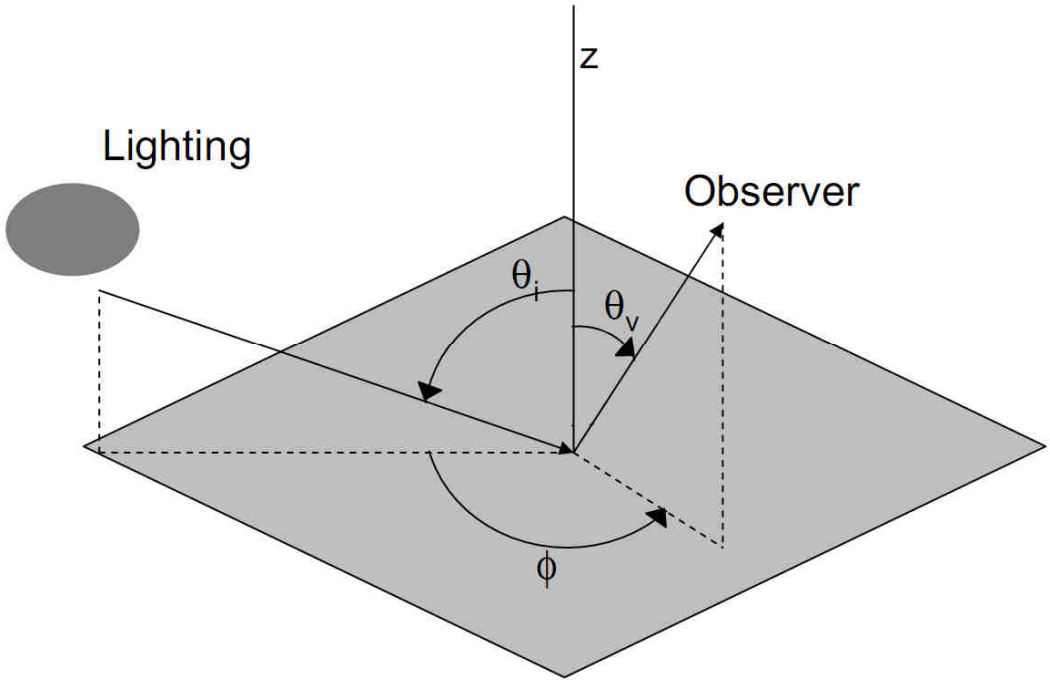

Figure 1 – Lighting and viewing configuration

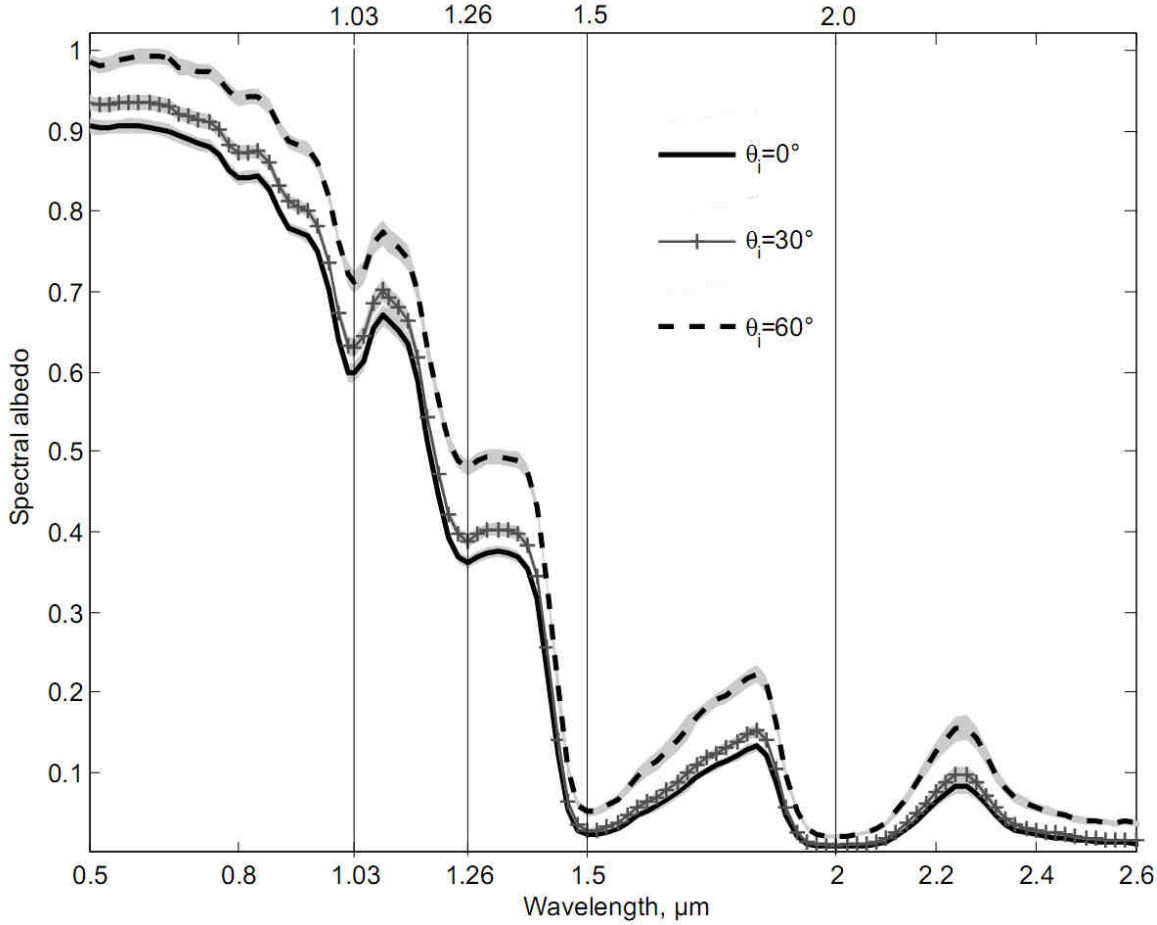

Figure 2- S3 spectral albedo α(λ,θi) calculated from BRDF measurements for three incident zenith angles. Vertical lines are located at spectral albedo minima. Gray areas represent an estimation of the uncertainties of albedo values due to interpolation and extrapolation of the measurements to the whole hemisphere. The uncertainties have been evaluated using SnowRAT and Mishchenko's models.

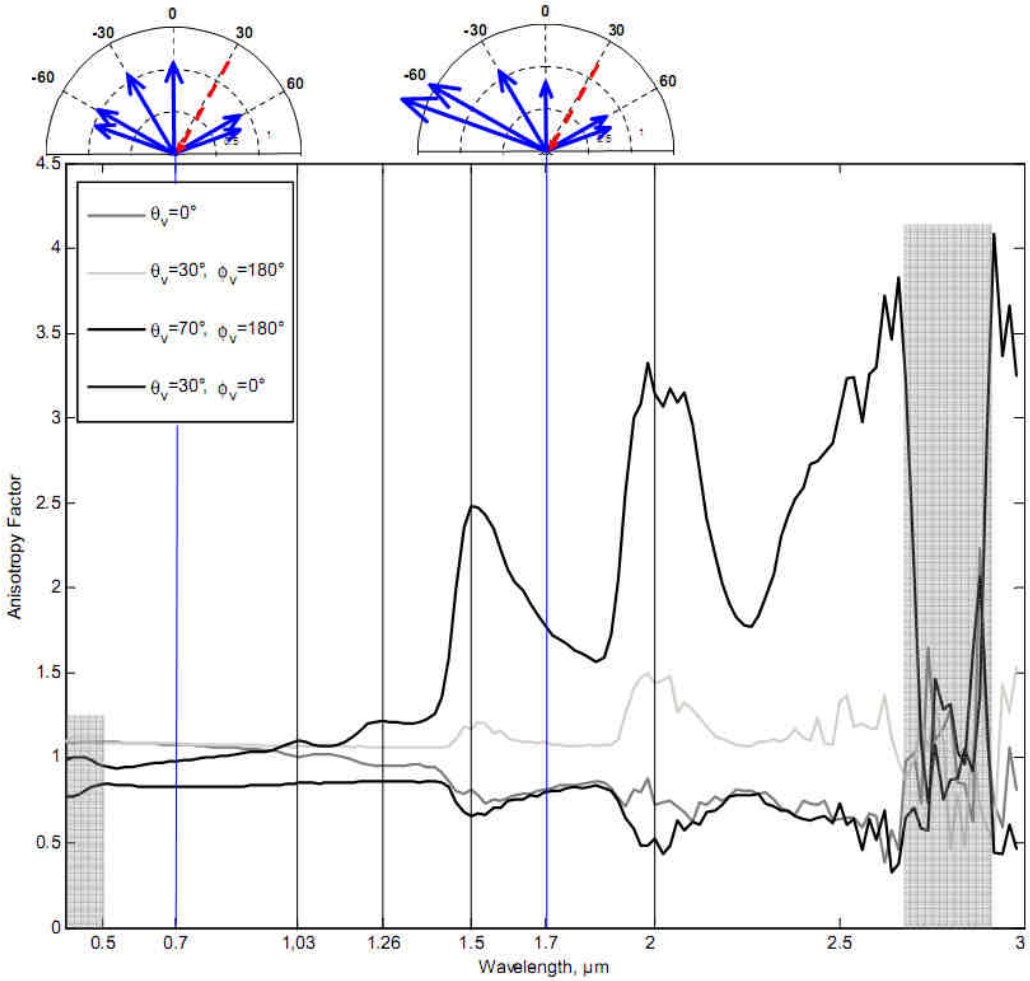

Figure 3 - S3 Anisotropy factor, R(λ) for different viewing angles in the principal plane. Incident angle is 30°. Vertical lines are the same as in Fig. 2. Gray areas correspond to wavelengths where photometric accuracy is reduced due to absorption by H_2O vapor or inaccurate calibration of the reference. Two polar plots in the principal plane, with all the measured viewing angles have been added at 0.7 and 1.7 μm above the chart.

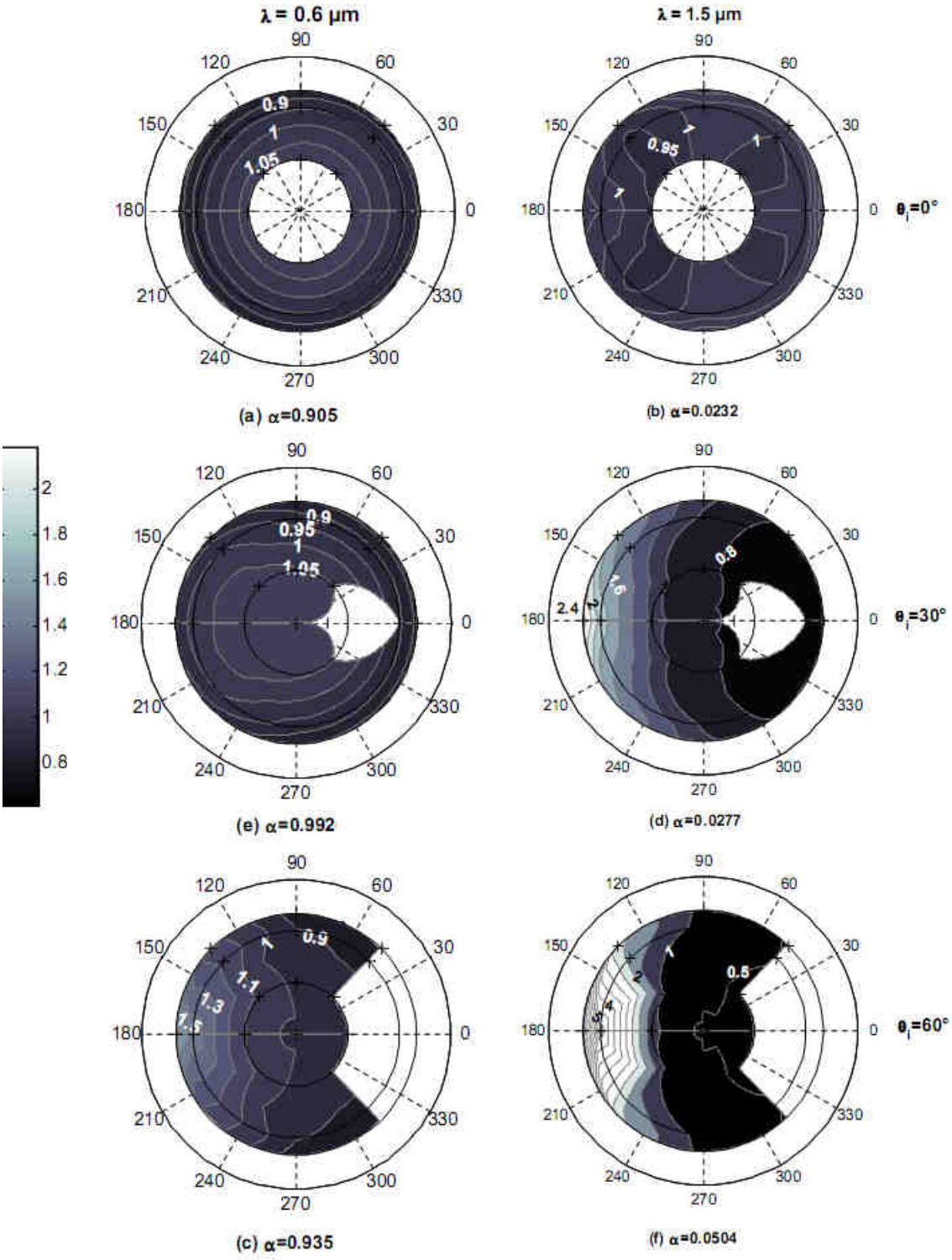

Figure 4 –S3 Anisotropy factor, R(θv ,φ), at 0.6 and 1.5 μm for zenith incident angles 0°, 30° and 60°. The polar angle corresponds to the relative azimuth, φ , between the viewing and the incident azimuth and the polar radius to the viewing angle, θv . The incident beam comes from the right and the forward direction is toward left. The three circles inside each plot represent viewing zenith angles of 30°, 60° and 70°. The crosses show the measurements used to generate the isolines. The spectral albedo used to calculate R is indicated below each chart.

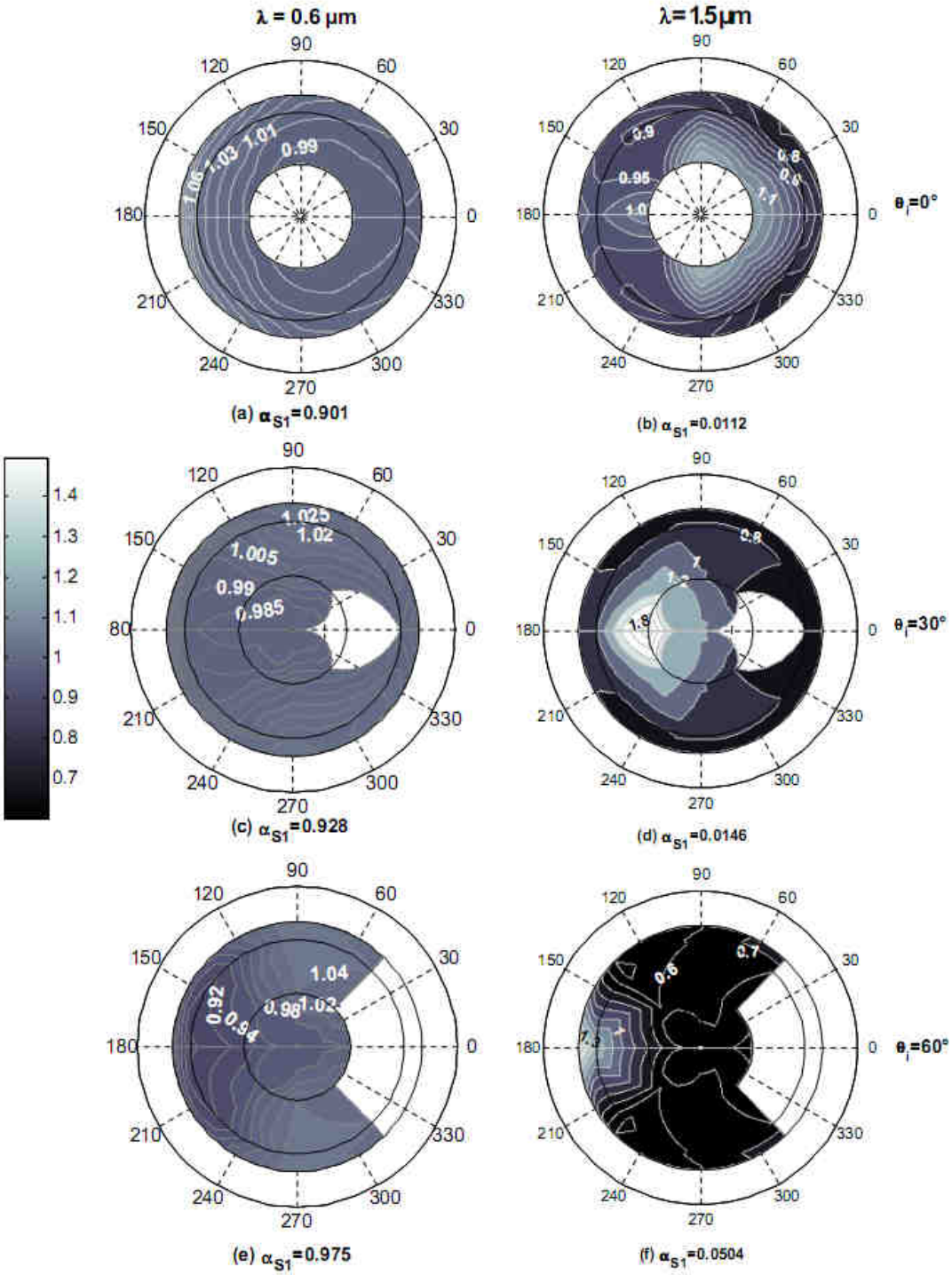

Figure 5- Ratio of the anisotropy factor R between samples S1 and S3 (R(S1)/R(S3)) at 0,30 and 60° incident beam and for two wavelengths. The spectral albedo used to calculate R for S1 is indicated below each chart. S3 spectral albedo is indicated in Figure 4.

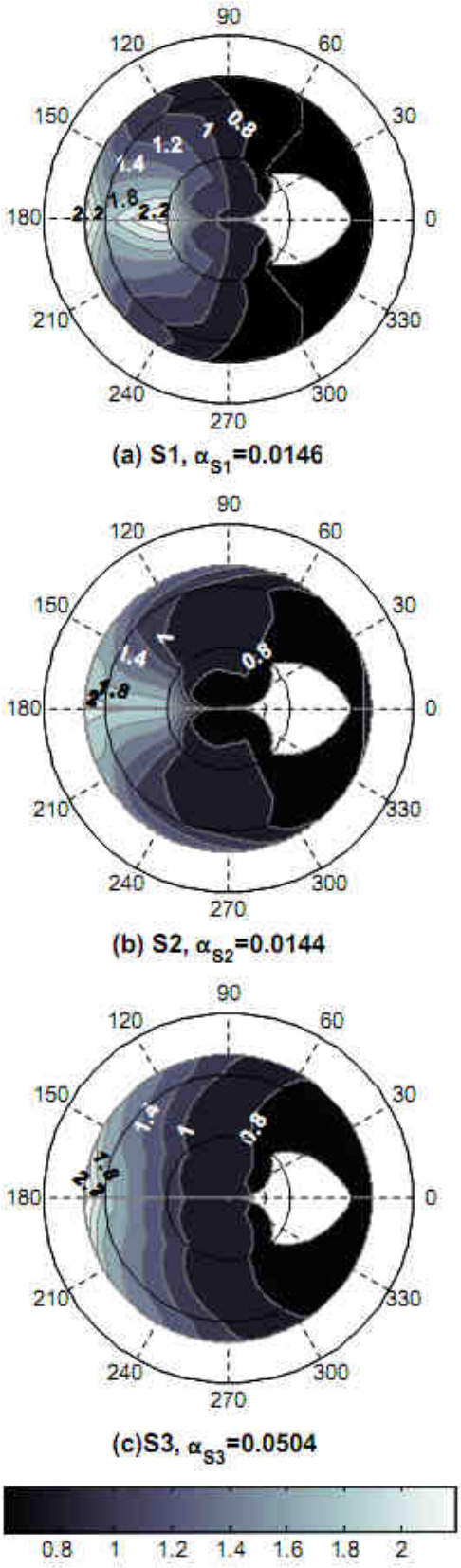

Figure 6 – Anisotropy factor R(θv ,φ) at 1.5 μm and θi=30°for three snow samples.

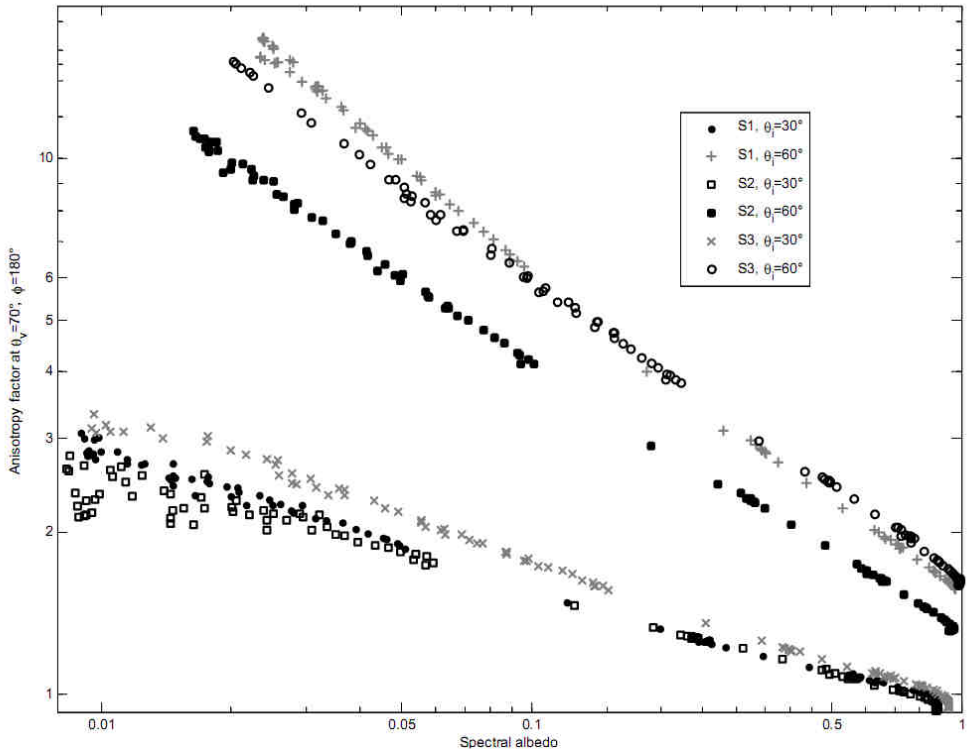

Figure 7 –Anisotropy factor R(θv=70°,φ=180°) versus spectral albedo (log-log plot) for the three samples and two incident angles (30°and 60°). Each point on the chart belongs to a wavelength for one sample and one incident zenith angle.

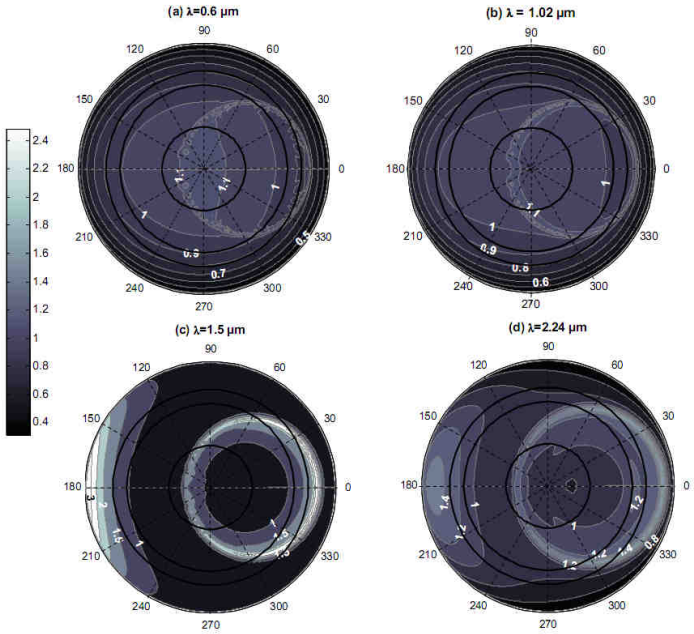

Figure 8 –Anisotropy factor R(θv,φ) (Mishchenko model, Mishchenko et al., 1999) for spheres with power law distribution of size. Incident angle is 30°. Effective radius is 0.1mm and effective variance of grain size distribution is 0.2 μm. Circles at 30°, 60° and 70° viewing angles are drawn on each polar chart.

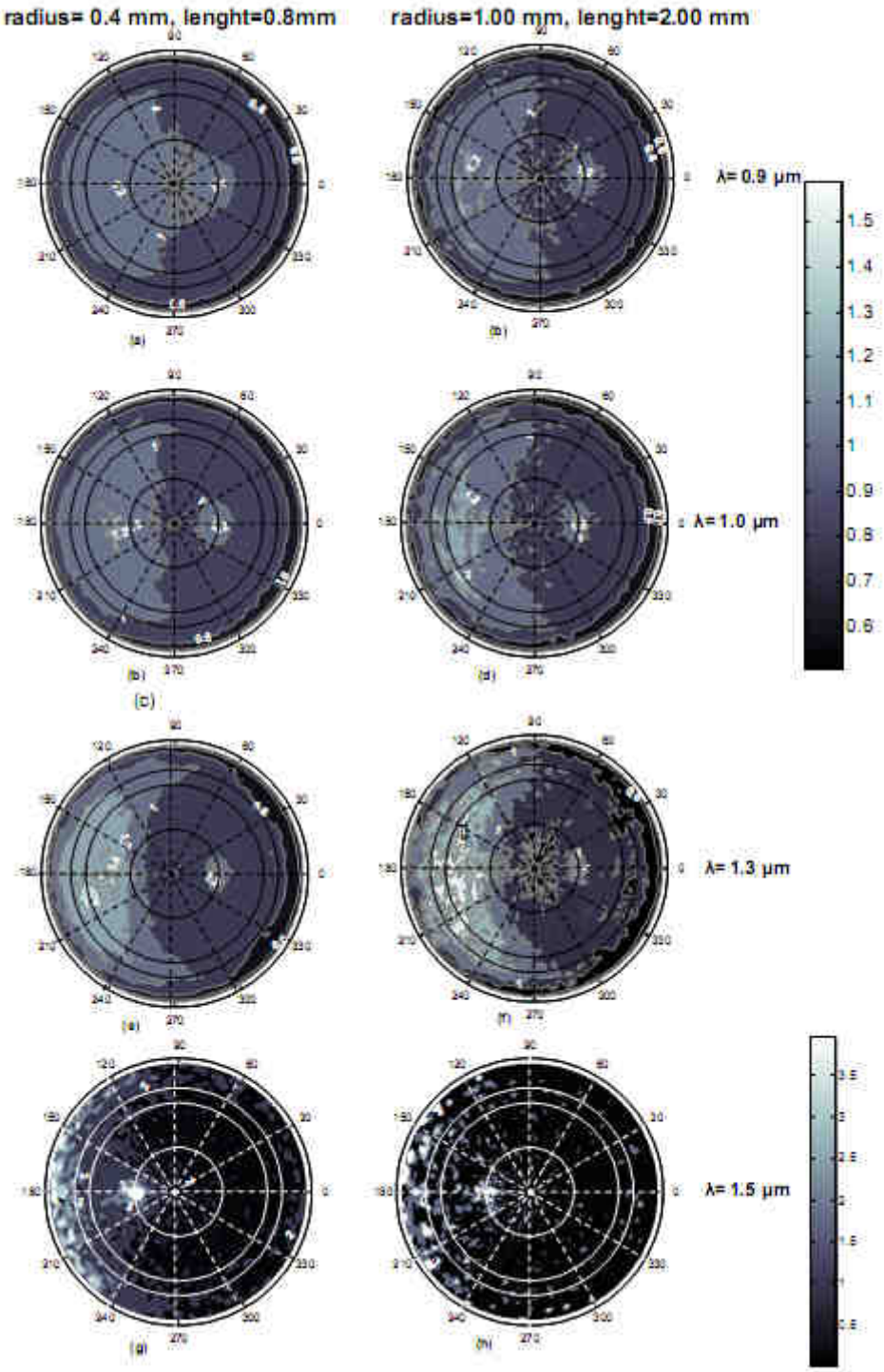

Figure 9 – Anisotropy factor R(θv,φ) computed with SnowRAT (Picard et al., 2008) for cylinders with random orientation. Incident angle is 30°. Circles at 30°, 60° and 70° viewing angles are drawn on each polar chart.